

A dual-color plasmonic focus for surface-selective four-wave mixing

Xuejun Liu, Yong Wang, and Eric O. Potma

Citation: *Appl. Phys. Lett.* **101**, 081116 (2012); doi: 10.1063/1.4747798

View online: <http://dx.doi.org/10.1063/1.4747798>

View Table of Contents: <http://apl.aip.org/resource/1/APPLAB/v101/i8>

Published by the [American Institute of Physics](#).

Related Articles

Digital optical phase conjugation of fluorescence in turbid tissue

Appl. Phys. Lett. **101**, 081108 (2012)

Phase control of bright and dark states in four-wave mixing and fluorescence channels

Appl. Phys. Lett. **101**, 081107 (2012)

All-optical time-stretch digitizer

Appl. Phys. Lett. **101**, 051113 (2012)

Origin of the oscillations in the self-diffracted signal in degenerate-two wave mixing experiment in azo-polymer

APL: Org. Electron. Photonics **5**, 121 (2012)

Origin of the oscillations in the self-diffracted signal in degenerate-two wave mixing experiment in azo-polymer

Appl. Phys. Lett. **100**, 233301 (2012)

Additional information on *Appl. Phys. Lett.*

Journal Homepage: <http://apl.aip.org/>

Journal Information: http://apl.aip.org/about/about_the_journal

Top downloads: http://apl.aip.org/features/most_downloaded

Information for Authors: <http://apl.aip.org/authors>

ADVERTISEMENT



HAVE YOU HEARD?

Employers hiring scientists
and engineers trust
physicstodayJOBS



<http://careers.physicstoday.org/post.cfm>

A dual-color plasmonic focus for surface-selective four-wave mixing

Xuejun Liu, Yong Wang, and Eric O. Potma^{a)}

Department of Chemistry, University of California, Irvine, California 92697, USA

(Received 19 June 2012; accepted 9 August 2012; published online 23 August 2012)

We describe a dual-color plasmonic lens suitable for focusing two femtosecond surface plasmon polariton wavefronts to a common focal spot. We show that the overlapping evanescent fields, which are confined to (sub-) micrometer dimensions, form a surface-selective excitation volume for four-wave mixing (FWM) experiments. We demonstrate that stable and virtually background-free FWM signals from single nano-objects placed in the plasmonic focus can be generated. The plasmonic focal spot constitutes a precisely controlled excitation source for surface-selective nonlinear spectroscopic measurements. © 2012 American Institute of Physics. [<http://dx.doi.org/10.1063/1.4747798>]

Four-wave mixing (FWM) is an optical technique that probes the third-order nonlinear optical response of materials. FWM is sensitive to both vibrational and electronic properties of materials, which has rendered the technique useful for a wide variety of applications. When combined with microscopic focusing, FWM can be used to examine the nonlinear optical properties of individual micro- and nano-structures. An example of FWM imaging is coherent anti-Stokes Raman scattering (CARS) microscopy,¹ which has found applications in biological imaging² as well as in the area of nanostructure characterization.³

The strong signals and high resolution in FWM microscopy arise from the capability to form a sub-micrometer sized excitation volume. This excitation volume results from the collinear overlap of the excitation beams, each focused to a diffraction-limited focal spot by the same high numerical aperture lens.⁴ The FWM excitation spot is typically confined to a three-dimensional volume of less than $1 \mu\text{m}^3$. The small size of the excitation volume produces high excitation densities, which boost FWM signal levels. In addition, the localized nature of focal spot reduces signal contributions from the bulk, and thus provides a mechanism for generating higher contrast from sub-micrometer sized objects.

In FWM studies of nanostructures, the targets are typically supported by glass substrates, which produce nonresonant FWM signals that often overwhelm the signal from the nanomaterial. To improve the FWM contrast from individual nanostructures, it would be highly beneficial to reduce the size of the focal volume even more, preferably to the size of the nanostructure itself, which would maximally suppress nonresonant contributions from the surrounding bulk or supporting medium. However, it is challenging to form nanoscopic FWM excitation volumes with free space light, as the size of the focal fields are dictated by the diffraction limit.

Alternatively, confined excitation fields can be attained when coupling freely propagating light to evanescent field modes at surfaces. This approach is utilized, for instance, in total internal reflection fluorescence (TIRF) microscopy, where fluorophores are excited only within the $\sim 100 \text{ nm}$

reach of the evanescent field at a glass surface.⁵ Another example is surface enhanced Raman scattering (SERS), which utilizes the highly localized and strong plasmonic fields at metal nanostructures for enhancing the weak Raman response of surface-tethered molecules.^{6,7} In both examples, the localized nature of the evanescent field suppresses bulk contributions and increases the signal contribution from the target compound in the vicinity of the surface. A similar approach has been used in FWM microscopy, including the use of metallic nanostructures to boost CARS signal levels from surface-tethered molecules^{8–11} and the use of flat gold surfaces to selectively excite structures near the metal interface.^{12–14}

Although the confined nature of plasmonic fields constitutes an attractive strategy for improving FWM contrast from nanoscopic objects, existing approaches lack the degree of control over excitation parameters that can be obtained with freely propagating light. Whereas in conventional FWM microscopy the excitation density and size of the focal volume are controllable parameters, the localized plasmonic fields at metallic nanostructures are often ill-defined. Controlled excitation conditions are important for FWM experiments in order to mitigate unwanted heating effects and spurious optical nonlinearities of plasmonic substrates. A higher level of control can be achieved when using the surface plasmon polariton (SPP) modes at flat metallic surfaces. However, the resulting evanescent fields are commonly not confined in the lateral dimension, thus, producing much lower FWM excitation densities.

In this work, we aim to combine the excellent surface-selective excitation properties of evanescent fields with the controlled confinement of diffraction-limited focal fields for the purpose of dual-color FWM microscopy. We achieve surface-selective FWM excitation by utilizing SPP excitation in a gold film, while making use of grating-based plasmonic lenses to confine the lateral focusing parameters. Previous work has shown that plasmonic lenses are capable of focusing SPP wavefronts to sub-wavelength spots.^{15–19} We here extend the use of such lenses into the regime of nonlinear optics. By using femtosecond pulses in a dual-color configuration, we show that a confined evanescent FWM excitation volume can be produced. Moreover, we demonstrate that

^{a)}epotma@uci.edu.

background-free FWM signals can be generated from nanoparticles (NPs) placed in such a plasmonic focus.

The FWM experiments described here are based on a dual-color CARS process, where incident frequencies ω_1 and ω_2 produce a signal frequency at $2\omega_1 - \omega_2$. The experimental layout is shown in Figure 1. The substrate consists of a 30 nm thick gold film, which contains two concentric half-circular plasmonic lenses. The lenses consist of grooves with a slit width of $0.15 \mu\text{m}$, fabricated with a focused ion beam (Quanta 3D FEG, FEI). The groove spacing in each of the lenses is tuned to optimize SPP excitation with the incident beams, 720 nm for λ_1 and 820 nm for λ_2 , corresponding to an inter-groove spacing of 698 nm and 805 nm , respectively. The radius of the inner half-circular slit is $5 \mu\text{m}$, and each lens consists of 10 concentric arcs. The lenses are placed in a parfocal geometry, forming a dual color plasmonic lens. In all experiments, the average power incident at the lens grating is less than 10 mW for each beam. For FWM experiments on nanoparticles, 30 nm sized Si particles (Meliorum Technologies) were first deposited on the gold surface. After identification of an isolated single Si nanoparticle, a plasmonic lens was milled around it, effectively positioning the particle at the center of the lens.

The optical excitation beams are derived from a Ti:sapphire laser (MaiTai, Spectra-Physics) and an optical parametric oscillator (Inspire, Spectra-Physics), producing pulses with a temporal width of 370 fs (λ_1) and 230 fs (λ_2) at the sample plane. The excitation beams are passed through 0.5 mm pinholes and imaged independently onto the back aperture of a high numerical aperture lens ($60\times$, NA 1.42 oil, Olympus). The shallowly focused excitation beams illuminate their respective side of the dual-color plasmonic lens at near normal incidence, forming each an $\sim 8 \mu\text{m}$ diameter illumination spot on the grating. Based on the size of the illu-

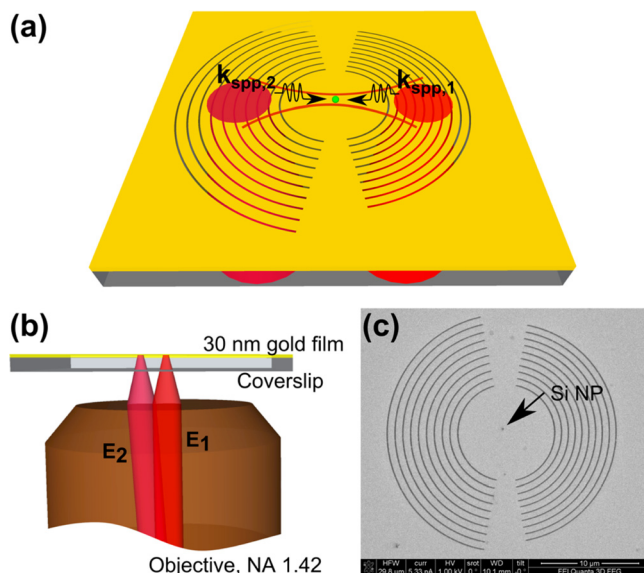


FIG. 1. (a) Excitation configuration for the dual-color plasmonic lens. Two independent SPPs are launched at each side of the plasmonic lens, and focused into a common focal spot, which is used for nonlinear excitation and probing of nanosized targets. (b) Geometry of objective-based illumination of incident fields E_1 and E_2 onto the dual-color plasmonic lens. (c) Scanning electron micrograph of a dual-color plasmonic lens and a Si nanoparticle (Si NP) target.

mination spots on the grating, the maximum focusing angle corresponds to $\sim 30^\circ$. The generated FWM and fluorescence emission from the sample are detected in the epi-direction by a charge-coupled device (CCD) camera (Clara, Andor) through a bandpass filter ($650/40 \text{ nm}$, Chroma). A dichroic mirror (680 SWP , Chroma) is used to separate the FWM emission from the incident light.

We first characterize the dimensions of the excitation field produced by the dual-color plasmonic focus. In Figure 2(a), a CCD image is shown of the plasmonic lens illuminated by the E_1 and E_2 excitation fields. Both fields couple to traveling SPPs in the film, producing SPP wavefronts that are focused at the center of the lens, as observed through the plasmon leakage radiation. The two SPP wavefronts, at frequency ω_1 and ω_2 , are counter-propagating and share a common focus. Due to interference effects in the film and in the imaging system, however, direct imaging of the fundamental SPP is not ideal for determining the size of the plasmonic focus. It also proves challenging to characterize the focal dimensions directly with FWM contrast, because the FWM of the gold surface as well as from bulk samples is suppressed in the counter-propagating excitation configuration.¹³

Instead, we use the two-photon excited fluorescence (TPEF) of rhodamine 6G in methanol, which is applied to the surface, as a contrast mechanism to visualize the nonlinear excitation spot. Although the TPEF signal exhibits a different dependence on the intensities of the incoming fields

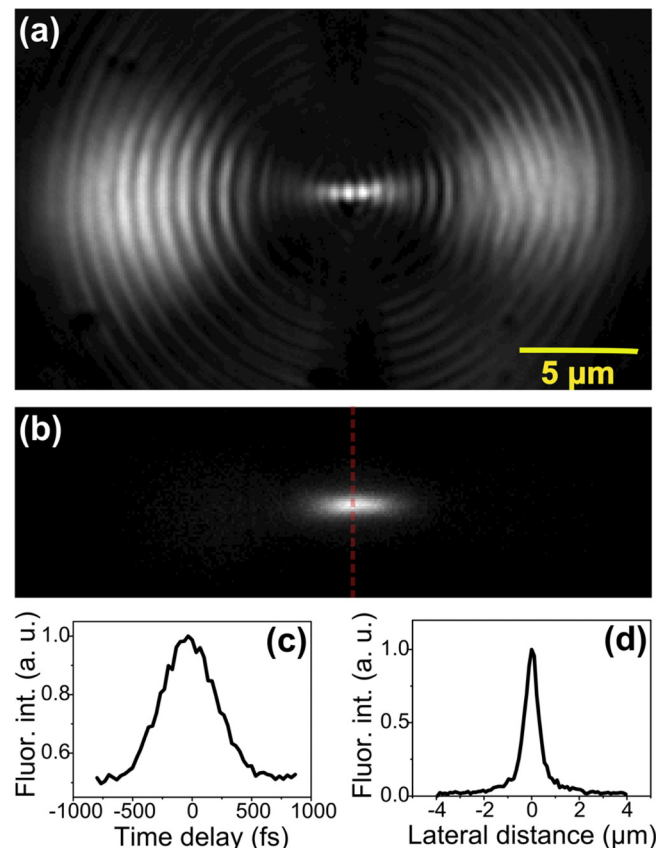


FIG. 2. (a) CCD image of the launching and focusing of two independent SPP modes with the plasmonic lens. (b) CCD image of the dual-color contribution ($\omega_1 + \omega_2$) to the TPEF of a R6G solution in methanol. (c) Dual-color TPEF signal as a function of the time delay between E_1 and E_2 . (d) Intensity profile of the dual-color TPEF signal along the vertical dashed line marked in (b), with a Gaussian FWHM of $0.63 \mu\text{m}$.

(2nd order) compared to FWM (3rd order), the use of TPEF allows for a direct inspection of the overlap area of the E_1 and E_2 foci. Figure 2(b) shows the contribution to the TPEF originating from one ω_1 photon and one ω_2 photon ($\omega_1 + \omega_2$). The dual-color TPEF image is obtained by subtracting images taken at zero time-delay and at a 1 ps time delay between the pulses. The temporal dependence of the dual-color TPEF contribution is plotted in Figure 2(c). The lateral full-width at half maximum (FWHM) of the dual-color focal spot is $0.63 \mu\text{m}$. Using a model for plasmonic focusing,¹⁹ we calculate that in the case of perfect parafocality, a lateral width of $0.48 \mu\text{m}$ is expected under these conditions. We attribute the discrepancy between the calculated and measured focal dimensions to non-perfect parafocality of the two SPP wavefronts due to possible spatial phase variations of the incident light beams. Such residual spatial phase gradients can be compensated by properly tailoring the transverse phase of the input beams with, for instance, spatial light modulators (SLMs). Note that, in principle, much tighter foci can be obtained by illuminating a larger area of the grating to achieve a higher effective NA of the lens.¹⁹ We have limited ourselves to a somewhat smaller illumination area here to achieve higher excitation densities with the laser power currently available with our system.

The confined dual-color plasmonic focus can be used to generate FWM signals from objects placed on the gold surface. In Figure 3(a), the FWM signal of a single Si nanoparticle positioned in the center of the plasmonic focus can be seen. The FWM from the nanoparticle is much stronger than any background contributions. Some residual TPEF from gold, excited by E_1 at the edges of the grooves of the lens, can be observed when changing the polarization of the incident light from P to S. However, as shown in Figure 3(b), these contributions are almost two orders of magnitude

weaker than the FWM signal seen in the plasmonic focus. We also note that the SPP-excited FWM signal does not blink and is stable for hours.

The strong FWM signals from nanoscopic objects in focus are generated without a loss of temporal resolution. In Figure 3(c), the FWM of a Si nanoparticle in focus is shown as a function of the time delay between E_1 and E_2 . The temporal width of the cross-correlation profile is identical to the convolution of the individual pulse widths, indicating that dispersion in the gold and spectral filtering at the lens are insignificant for excitation pulses in the 200 fs range used here. The limited influence of spectral filtering is also demonstrated in Figure 3(d), where the FWM generation efficiency in focus is plotted as a function of λ_1 . The spectral tolerance of the lens grating is sufficient to accommodate coupling of ~ 200 fs incident pulses into a SPP wavefront in the gold film without compromising the pulse spectrum.

In summary, in this work, we demonstrate that plasmonic lenses are suitable for nonlinear optical experiments. We use a dual-color lens design that forms an evanescent focus capable of generating localized TPEF and FWM signals. The evanescent excitation field limits the generation of FWM signals to within the first ~ 100 nm away from the surface,¹⁴ rendering this approach suitable for surface selective measurements. Although the field confinement in these nonlinear excitation spots is less than what can be achieved at plasmonic tips and at engineered nanostructures, the plasmonic lens offers a much higher degree of controllability of electric field parameters akin to the situation in the 3D foci of free space light. Under the controlled conditions of location and spatial field confinement, we obtain SPP-excited FWM signals of single nano-objects. The femtosecond FWM signals in focus retain a high

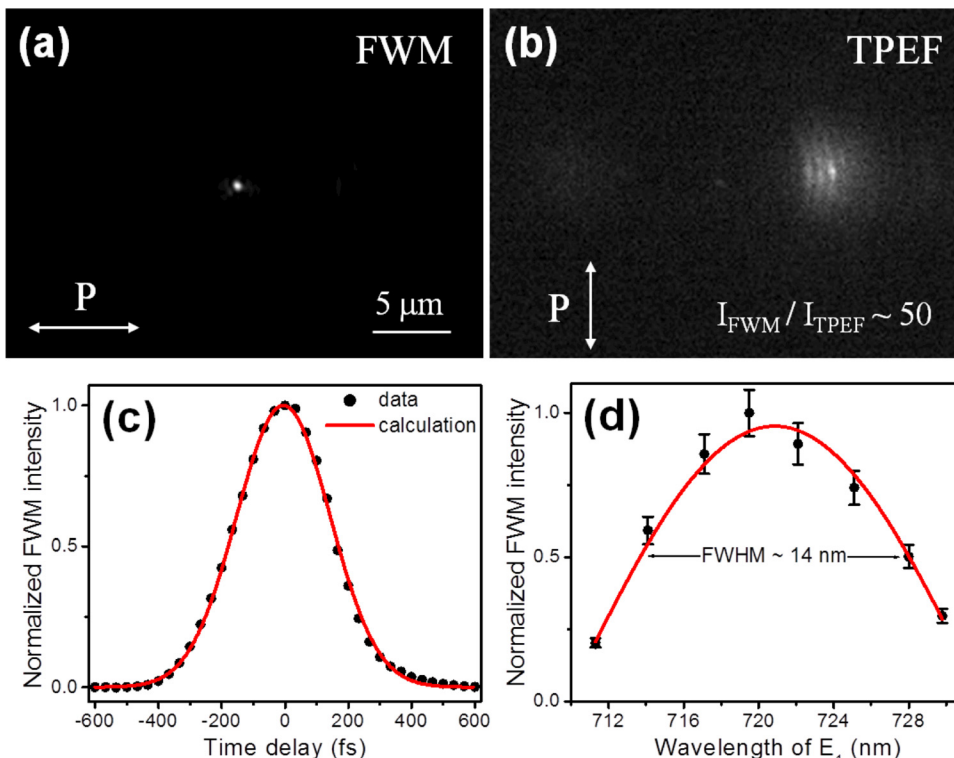


FIG. 3. CCD image of FWM radiation from a Si nanoparticle at the focus of a dual-color plasmonic lens, with incident light polarized parallel (a) and perpendicular (b) to the optical axis of the lens. (c) FWM signal as a function of the time delay between E_1 and E_2 . The solid curve is the calculated cross-correlation based on the (Gaussian) pulse widths of the incident pulses. (d) Dependence of the FWM signal on λ_1 . The solid curve is a guide to the eye.

temporal resolution, are stable, and are virtually free of spurious background contributions.

We anticipate that the plasmonic FWM focus has many interesting applications. For instance, by applying an appropriate spatial phase shift on the incident fields with spatial light modulators, it is possible to translate the excitation volume laterally and along the optical axis of the lens, constituting a 2D analog of a laser scanning FWM microscope. The confined evanescent FWM probing volume is also useful for high-precision, surface-selective nonlinear spectroscopy measurements of individual nanostructures or molecules. In particular, the localized FWM excitation field is attractive for FWM correlation spectroscopy measurements.²⁰ Given that the plasmonic lens performs well even when exposed to liquids, the surface-selective FWM probing volume offers an opportunity to carry out sensitive correlation spectroscopy measurements of interfacial chemical interactions.

This work is supported by the Department of Energy, Grant No. DE-SC0003905. We are also thankful to the Center of Chemical Innovation, National Science Foundation, Grant No. CHE-0802913, for providing access to instrumentation.

¹A. Zumbusch, G. R. Holtom, and X. S. Xie, *Phys. Rev. Lett.* **82**, 4142 (1999).

²C. L. Evans and X. S. Xie, *Annu. Rev. Anal. Chem.* **1**, 883 (2008).

- ³Y. Wang, C.-Yu. Lin, A. Nikolaenko, V. Raghunathan, and E. O. Potma, *Adv. Opt. Photon.* **3**, 1 (2011).
- ⁴J. X. Cheng, A. Volkmer, and X. S. Xie, *J. Opt. Soc. Am. B* **19**, 1363 (2002).
- ⁵D. Axelrod, T. P. Burghardt, and N. L. Thompson, *Annu. Rev. Biophys. Bioeng.* **13**, 247 (1984).
- ⁶M. Fleischmann, P. J. Hendra, and A. J. McQuillan, *Chem. Phys. Lett.* **26**, 163 (1974).
- ⁷M. Moskovits, *Rev. Mod. Phys.* **57**, 783 (1985).
- ⁸H. Chew, D. S. Wang, and M. Kerker, *J. Opt. Soc. Am. B* **1**, 56 (1984).
- ⁹T. Ichimura, N. Hayazawa, M. Hashimoto, Y. Inouye, and S. Kawata, *J. Raman Spectrosc.* **34**, 651 (2003).
- ¹⁰V. Namboodiri, M. Namboodiri, G. I. Cava-Diaz, M. Oppermann, G. Flacheneker, and A. Materny, *Vib. Spectrosc.* **56**, 9 (2011).
- ¹¹C. Steuwe, C. F. Kaminski, J. J. Baumberg, and S. Mahajan, *Nano Lett.* **11**, 5339 (2011).
- ¹²C. K. Chen, A. R. B. de Castro, and Y. R. Shen, *Phys. Rev. Lett.* **43**, 946 (1979).
- ¹³X. Liu, Y. Wang, and E. O. Potma, *Opt. Lett.* **36**, 2348 (2011).
- ¹⁴Y. Wang, X. Liu, A. R. Halpern, K. Cho, R. M. Corn, and E. O. Potma, *Appl. Opt.* **51**, 3305 (2012).
- ¹⁵Z. W. Liu, J. M. Steele, W. Srituravanich, Y. Pikus, C. Sun, and X. Zhang, *Nano Lett.* **5**, 1726 (2005).
- ¹⁶L. L. Lin, V. K. Vlasko-Vlasov, J. Pearson, J. M. Hiller, J. Hua, U. Welp, D. E. Brown, and C. W. Kimball, *Nano Lett.* **5**, 1399 (2005).
- ¹⁷J. M. Steele, Z. Liu, Y. Wang, and X. Zhang, *Opt. Express* **14**, 5664 (2006).
- ¹⁸Z. Liu, J. M. Steele, H. Lee, and X. Zhang, *Appl. Phys. Lett.* **88**, 171108 (2006).
- ¹⁹J. T. Banhs, A. Imre, V. K. Vlasko-Vlasov, J. Pearson, J. M. Hiller, L. H. Chen, and U. Welp, *Appl. Phys. Lett.* **91**, 081104 (2007).
- ²⁰J. X. Cheng, E. O. Potma, and X. S. Xie, *J. Phys. Chem. A* **106**, 8561 (2002).